DR SEAN REGAN (Orcid ID : 0000-0002-8445-5138)

DR JEFFREY A BENOWITZ (Orcid ID : 0000-0003-2294-9172)

Article type : Paper

A plutonic brother from another magma mother: disproving the Eocene Foraker-McGonagall pluton piercing point and implications for long-term slip on the Denali Fault

Sean P. Regan[1], Jeff A. Benowitz[2], and Mark E. Holland[3]

1. *Dept of Geosciences, University of Alaska Fairbanks, Fairbanks AK 99775*
2. *Geophysical Institute, University of Alaska Fairbanks, Fairbanks AK 99775*
3. *Department of Life, Earth, and Environmental Sciences, West Texas A&M University, Canyon, TX, 79016*

Corresponding author: Sean Regan, sregan5@alaska.edu; (907) 474-5386

Abstract

The Denali Fault is an active strike-slip fault system responsible for the highest topography in North America, yet there are conflicting constraints on the fault's Cenozoic slip history. The long-term slip rate constraint of the eastern Denali Fault is ~400 km since 57 Ma. In apparent conflict, the long-term slip rate of the western Denali Fault is 38 km since 38 Ma based on the reconstruction of the Foraker and McGonagall plutons. Tests of the genetic relationship of the plutons with bulk rock geochemical and paired U-Pb and Hf zircon analysis suggest a disparate origin. The McGonagall pluton, despite having a lower SiO_2, has lower ε_{Hf} values inconsistent with chemical and isotopic variations between the two being the result of contamination. The Denali Fault is a highly strain partitioned system, but the amount of Cenozoic slip dispersed west to east is likely significantly less than the previous ~360 km constraint.

This article has been accepted for publication and undergone full peer review but has not been through the copyediting, typesetting, pagination and proofreading process, which may lead to differences between this version and the Version of Record. Please cite this article as doi: 10.1111/TER.12437

Keywords: Denali Fault, Alaska, piercing point, fault plutonism, Hf in zircon, geochemistry

INTRODUCTION

Strike-slip faults across the globe take up a significant portion of plate convergence (Molnar and Dayem, 2010) and can translate crustal blocks 100's of kms over 10's of millions of years. Hence, constraining the amount of offset on major strike-slip faults is fundamental to both understanding near fault process and the transfer of strain inboard from plate boundaries. However, establishing robust piercing points across lithospheric-scale strike slip faults is often fraught with conflicting results (Umhoefer, 2000) as different geologic features yield disparate reconstructions. Commonly utilized features include Large Igneous Provinces (Mahan and Williams, 2005; Ernst and Bleeker, 2010), dismembered plutons (Frizzell et al., 1986; James, 1992; Darin and Dorsey, 2013), general lithologic correlation (Sutherland et al., 2013), basin reconstruction, and paleomagnetism (Umhoefer, 2000; Hildebrand, 2015).

Chief among these constraints is the use of tectonically fragmented plutons, though they have fueled much debate in some of the classic strike slip faults around the world including the San Andreas (Frizzell et al., 1986; Powell, 1993) and the Karakorum (Phillips et al., 2013). Application of the commonly used "same-pluton" method for fault reconstruction is complicated by our understanding of fault zones facilitating the transport of igneous material through the crust (Tikoff and Teyssier, 1992; Roman-Berdiel et al., 1997; Rosenberg, 2004), and requires distinguishing distinct plutons of similar age and character emplaced along a fault from a true tectonically fragmented pluton. Consequently, a rigorous petrographic, geochemical, and isotopic approach evaluating the genetic relationship of fault-bound plutons is central to efforts aimed at constraining fault offset.

THE DENALI FAULT AND THE ALASKA RANGE

The >2000 km long intracontinental Denali Fault in the northern Cordillera is a lithospheric-scale strike-slip fault demonstrated by a >10 km Moho offset (Allam et al., 2017). The modern Denali Fault is a highly strain partitioned system, with thrust fault splays on both sides of the Fault (Bemis et al., 2015; Burkett et al., 2016; e.g. Waldien et al., 2018) and takes up to ~20% of the convergence rate of the Pacific-Yakutat plates with North America (Elliot et al., 2013). As such, the Denali Fault poses one of the greatest seismic hazards in North America exemplified by the 2002 M_w 7.9 Denali earthquake, which catalyzed a surface rupture exceeding 340 km in length (Hreinsdottir et al., 2003). Cenozoic motion along and adjacent to the Denali Fault system has resulted in the dramatic topography of the Alaska Range (>6 km relief), focused arc magmatism (Berkelhammer et al., 2019; Brueseke et al., 2019), and caused a transient but extreme exhumation history for rocks proximal to the fault zone (Fitzgerald et al., 1995; Riccio et al., 2014; e.g. Waldien et al., 2018; Benowitz et al., 2019).

Total offset and average slip rates across the Denali Fault have remained a contentious topic owing to multi-disciplinary datasets pointing to different east to west modern and ancient slip rates (Lowey, 1998; Haeussler et al., 2017). Net slip estimates to the east include 370 km of post-Cretaceous slip based on correlation of carbonate megaboulders to their source (Lowry, 1998) and >400 km of post 57 Ma slip based on terrane correlation (Fig. 1)(e.g. Nokleberg et al., 1985; Ricco et al., 2014). These eastern Denali Fault estimates yield an average slip rate of 7 mm/yr since ~57 Ma. In contrast, the reconstruction of the ca. 38 Ma Foraker and McGonagall plutons to the west (Figs. 1 and 2) suggest 38 km of net slip (Fig. 2; Reed and Lanphere, 1974). Reconstruction of these two plutons establishes an average slip-rate of 1 mm/yr.

Cosmogenic exposure dating of offset glacial features constrains Pleistocene right-lateral motion on the Denali Fault to ~14 mm/yr within the eastern Alaska Range and 5 mm/yr along the western edge of the assumed Foraker pluton (Fig. 1) (Haeussler et al., 2017), consistent with decreasing slip from east to west along the Denali Fault. In addition, rigorously-scaled analogue modelling (Toenenboehn et al., 2018) paired with high-resolution thermochronology (Fitzgerald et al., 1995, Lease et al., 2016; Burkett et al., 2016) studies demonstrates that the current restraining bend geometry and resultant localized uplift of Mount Denali could be accommodated almost entirely within the last six million years indicating significant strike-slip motion during this time period. As new studies employing a wide variety of analytical approaches through space and time converge on higher slip rates for the western Denali Fault, the validity of the oft-cited Foraker-McGonagall 1 mm/yr piercing point comes into question (Fig. 3).

TESTING THE FORAKER-MCGONAGALL PIERCING POINT

To evaluate the validity of the Foraker-McGonagall piercing point, we present a combined dataset (DR1) of U-Pb zircon geochronology, Hf-isotope analysis, and bulk rock geochemistry. We present detrital zircon U-Pb geochronologic data from catchments that drain the Foraker and McGonagall plutons. The combined bedrock-detrital approach provides unmatched insight into the age and petrogenesis of each pluton.

Petrographic analyses of each pluton display intrapluton consistency, but differences between the two plutons. As noted by Reed and Lanphere (1974), the Foraker pluton contains greater modal K-feldspar (perthitic) and reddish biotite (Fig. 4), whereas the McGonagall pluton is composed mostly of well-zoned plagioclase feldspar, quartz, matrix K-feldspar, biotite, and local hornblende. The two plutons have limited overlap with respect to major element composition (*for geochemical data see DR2*), with samples from the Foraker pluton ranging from 68.4 – 73.7 wt % SiO_2, with only one sample below 70.0 wt% while the McGonagall ranges from 66.0 – 70.3 wt %SiO_2 (Fig. 5a,b). REE patterns normalized to primitive mantle for the McGonagall pluton have steep LREE and MREE slopes with flat HREE concentrations (Fig. 4c) and high Sr and low Y and Yb concentrations (Fig. 5d), similar to crustal-derived adakitic rocks from the Lhasa Terrane in India (Shui et al., 2018). In contrast, the Foraker pluton has steep LREE patterns with large negative Eu anomalies, and relatively flat HREE.

Detrital zircon U-Pb geochronology from modern river sediments provides a spatially representative sampling of each pluton (*see DR3*). Detrital zircon from an isolated catchment draining the McGonagall pluton (n = 68; Muldrow glacier) were analyzed via LA-ICP-MS and compared with existing and new detrital U-Pb data from Yenta and Kahiltna catchments presented in Lease et al. (2016) (n = 94; Foraker pluton) in an attempt estimate the range of ages present in each pluton. Catchments receiving detritus from the Foraker pluton yield a weighted Eocene average of 36.5 ± 0.3 Ma (33.88 – 39.96 Ma), in comparison to detrital zircon from the Muldrow catchment sourced from the McGonagall pluton, which is older (39.2 ± 0.4 Ma; range: 36.50 – 45.67 Ma) (Fig. 2b). Detrital zircon U/Th ratios are also systematically different between the two datasets where zircon from Yentna and Kahiltna catchments yielded average U/Th ratios of 4.1 (2σ=3.2) relative to Eocene zircon detritus from the Muldrow catchment (average U/Th = 2.8; 2σ=1.4).

Paired U-Pb and Hf-isotope analysis on zircon (*see DR4*) was performed on four samples from along each pluton to establish upper and lower bounds on crystallization, to assess gradients that may help decipher pluton zonation, and to evaluate the role of contamination that may have modified bulk compositions. All zircon analyzed in this study are relatively homogeneous, often displaying oscillatory zoned doubly-terminated prismatic morphologies (Fig. 6a). One existing SHRIMP dataset presented in Hung (2008) from the Foraker pluton yielded a $^{206}Pb/^{238}U$ weighted mean of 37.2 ± 0.3 (MSWD: 1.8; Fig. 2 for location). Four additional samples were analyzed and presented herein. Two samples yielded tightly clustered $^{206}Pb/^{238}U$ weighted averages consistent with results in Hung (2008; 37.93 ± 0.42 Ma and 37.59 ± 0.36 Ma; Fig. 6b,c), which young from east to west. The other two samples from the western portion of the Foraker pluton yielded Paleocene ages ($^{206}Pb/^{238}U$ weighted averages: 58.45 ± 0.72 and 58.86 ± 0.60 Ma; Fig. 6b) and indicate that some portions of the western Foraker pluton belong to the older McKinley sequence of granitoids (Lanphere and Reed, 1985; Hung, 2008). Samples from the McGonagall pluton have $^{206}Pb/^{238}U$ weighted average ranging from 42.39 ± 0.34 Ma in the west to 38.78 ± 0.23 Ma in the east, with all samples consistently decreasing in age from the western end of the pluton to the east (Fig. 6d). Data from the two plutons indicate no overlap in crystallization ages, opposing younging trajectories, and suggest that portions of the western Foraker pluton are not Eocene, but rather belong to an older and more widespread magmatic event in the Alaska Range.

Hf-isotope analyses indicate that both the Foraker and McGonagall plutons have $\varepsilon_{Hf(t)}$ values slightly below contemporaneous depleted mantle, and well above CHUR (Fig. 7). However, the McGonagall pluton has somewhat lower $\varepsilon_{Hf(t)}$ values (+5.5 to+10.3) than the Foraker pluton samples (+9.7 to+14.0). These results are consistent with intrusion of the McGonagall pluton on the North America side of the Denali Fault, where North American lithosphere is more isotopically evolved, but are inconsistent with the Foraker-McGonagall reconstruction. If compositional variations were the result of contamination distribution in a once coherent pluton, lower $\varepsilon_{Hf(t)}$ values would be predicted in the more compositionally evolved (higher SiO_2, K_2O, and less Al_2O_3) pluton. However, our geochemical data indicate that the Foraker pluton is more compositionally evolved than the McGonagall pluton. Therefore, the dataset generated by our combined approach make the Foraker-McGonagall pluton correlation untenable.

IMPLICATIONS FOR LONG TERM SLIP ON THE DENALI FAULT

The three-dimensional structure and corresponding Moho offset of the Denali Fault are inconsistent with suggested primarily vertical-motion to explain relatively minor (<40 km) apparent strike-slip separation since the late Eocene (Csejtey et al., 1982; Mezger et al., 1997), as normal and reverse faults generally shallow with increasing depth. Structural analysis and sedimentology of early Cenozoic basins indicate deposition synchronous with right-lateral motion beginning after final collision of the Wrangellia Composite Terrane at ca. 60 Ma (Cole et al., 1999; Ridgeway et al., 2002). Eocene – Oligocene basin development is preserved on both sides of the Denali Fault and corresponding stratigraphic relationships are consistent with predominately strike-slip motion along the Denali Fault since the Eocene (Trop et al., 2004, 2019). Fabric analysis paired with piercing point reconstructions, syn-kinematic dike swarms, thermochronologic data, and offset glacial features require continual dextral motion from ~30 Ma to present (Benowitz et al., 2011;2012a,2014, 2019; Riccio et al., 2014; Burkett et a.., 2016; Lease et al., 2016; Tait, 2017; Haeussler et al., 2017; Waldien et al., 2018; Trop et al., 2019). These interdisciplinary data in totality are consistent with predominately right-lateral strike slip motion along the Denali Fault throughout the Cenozoic to the present.

Total Cenozoic displacement along the Denali Fault remains a critically unresolved question in North American Cordilleran tectonics. Establishing robust piercing points and questioning long-standing slip limiting constraints with modern tools adds insight to our understanding of strain partitioning along strike-slip faults (Burkett et al., 2016), Baja-Alaska models of large-scale translation of geologic features (Garver and Davidson, 2015), and the transfer of slip from the plate margin interface inboard (Elliot et al., 2013). The long-held Foraker-McGonagall pluton reconstruction has limited the amount of allowable Cenozoic offset across the Denali Fault to no more than 38 km since ~38 Ma (Reed and Lanphere, 1974) calling into question the role a ~2000 km long lithospheric-scale structural feature has played in the Cenozoic history of North American Cordilleran tectonics. However, new U-Pb and Hf-isotope data, and bulk-rock major and trace element chemistry confirm that this oft-cited piercing point is no longer tenable. Rather, the Foraker and McGonagall plutons have disparate origins, emplaced as two separate plutonic bodies along the Denali Fault.

Removing this long-held constraint reinforces the viability of continuous strike-slip motion on the Denali Fault since ~57 Ma (Nokleberg et al., 1985; Riccio et al., 2014; Burkett et al., 2016; Haeussler et al., 2017; Trop et al., 2019). Based on the now invalidated Foraker-McGonagall piercing point, the amount of Cenozoic net slip decrease east to west is likely significantly less than the previous assumed ~360 km of missing slip. It has been suggested that slip rates on the Denali Fault, based on thermochronology analysis, have been consistent since ~25 Ma (Benowitz et al., 2014) which correlates with a newly defined change in Pacific plate motion (Jicha et al., 2018). Pleistocene rates to the east (~14 mm/yr) lead to ~350 km of offset extrapolated since ~25 Ma and Pleistocene rates to the west (~5 mm/yr) lead to ~125 km of offset since ~25 Ma. The east to west Denali Fault offset difference since ~25 Ma is ~225 km. These time averaged rates are remarkably similar to those obtained from other suggested geologic piercing points (Fig. 1) (West: ~150 km since ~29 Ma, Trop et al., 2019; East: ~300 km since ~25 Ma, Benowitz et al., 2012b; East: ~80 km since ~6 Ma; Waldien et al., 2018). The structures responsible for and the mechanics of the ~225 km of missing Neogene Denali Fault slip remains an open question, but thrust splays off the south side of the fault (Riccio et al., 2014; Haeussler et al., 2017) and dip-slip motion along the master Denali Fault strand (Benowitz et al., 2011) clearly play a significant role.

Our overall workflow involving a spatially representative geochemical, geochronologic, and isotopic dataset is a robust method to distinguish discrete plutons of similar age and character from a once coherent pluton that was tectonically dismembered. In particular, the combination of a modern river catchment zircon U-Pb zircon detrital approach to better capture a large pluton's construction history with higher precision zircon U-Pb dating of bedrock samples allows for a more complete testing of the genetic relationship between pluton emplaced along a strike-slip fault.

ACKNOWLEDGEMENTS

NSF provided partial funding support through EAR# 1249885 awarded to Jeff Benowitz. Analytical support was provided by University of Alaska, Fairbanks. Peyton Presler is thanked for initial petrographic work. We would like to thank Mark Pecha, Daniel Alberts, Dominque Geisler, the rest of the Arizona Laserchron Center crew, Jeff Chiarenzelli, and Marian Lupulescu. The clarity of the manuscript was improved by reviews by Terry Pavlis, Paul Umhofer, and an anonymous reviewer.

DATA AVAILABILITY STATEMENT

We present a combined dataset in the supplementary material.

REFERENCES

Allam, A.A., Schulte-Pelkum, V., Ben-Zion, Y., Tape, C., Ruppert, N. and Ross, Z.E., 2017. Ten kilometer vertical Moho offset and shallow velocity contrast along the Denali fault zone from double-difference tomography, receiver functions, and fault zone head waves. Tectonophysics, *721*, pp.56-69.

Bemis, S.P., Weldon, R.J. and Carver, G.A., 2015, Slip partitioning along a continuously curved fault: Quaternary geologic controls on Denali fault system slip partitioning, growth of the Alaska Range, and the tectonics of south-central Alaska. Lithosphere, 7(3), pp.235-246.

Benowitz, J.A., Davis, K. and Roeske, S., 2019, A river runs through it both ways across time: 40Ar/39Ar detrital and bedrock muscovite geochronology constraints on the Neogene paleodrainage history of the Nenana River system, Alaska Range. Geosphere, 15(3), pp.682-701.

Benowitz, J.A., Layer, P.W. and Vanlaningham, S., 2014. Persistent long-term (c. 24 Ma) exhumation in the Eastern Alaska Range constrained by stacked thermochronology. Geological Society, London, Special Publications, 378(1), pp.225-243.

Benowitz, J. A., Vansant, G., Roeske, S., Layer, P. W., O'Sullivan, P.B. & Hults, C. P. 2012a. Geochronological constraints on the Eocene to Present slip rate history of the Eastern Denali Fault System. Geological Society of America Abstracts with Programs, 44, 634.

Benowitz, J.A., Layer, P.W., Armstrong, P., Perry, S.E., Haeussler, P.J., Fitzgerald, P.G. and VanLaningham, S., 2011. Spatial variations in focused exhumation along a continental-scale strike-slip fault: The Denali fault of the eastern Alaska Range. Geosphere, 7(2), pp.455-467.

Berkelhammer, S.E., Brueseke, M.E., Benowitz, J.A., Trop, J.M., Davis, K., Layer, P.W. and Weber, M., 2019, Geochemical and geochronological records of tectonic changes along a flat-slab arc-transform junction: Circa 30 Ma to ca. 19 Ma Sonya Creek volcanic field, Wrangell Arc, Alaska. Geosphere.

Brennan, P.R. and Ridgway, K.D., 2015. Detrital zircon record of Neogene exhumation of the central Alaska Range: A far-field upper plate response to flat-slab subduction. Bulletin, 127(7-8), pp.945-961.

Brueseke, M.E., Benowitz, J.A., Trop, j.M., Davis, K.N., Berkelhammer, S.E., Layer, P.W., and Morter, B.K., 2019, The Alaska Wrangell Arc: ~30 Ma of subduction-related magmatism along a still active arctransform junction: Terra Nova, v. 31, p. 59-66.

Burkett, C.A., Bemis, S.P. and Benowitz, J.A., 2016. Along-fault migration of the Mount McKinley restraining bend of the Denali fault defined by late Quaternary fault patterns and seismicity, Denali National Park & Preserve, Alaska. Tectonophysics, 693, pp.489-506.

Cole, R.B., Ridgway, K.D., Layer, P.W., and Drake, J., 1999, Kinematics of basin development during the transition from terrane accretion to strike-slip tectonics, Late Cretaceous-early Tertiary Cantwell Formation, south central Alaska: Tectonics, v. 18, p. 1224-1244.

Csejtey Jr, B., Ford, A.B., Yeend, W.E. and Wrucke, C.T., 2011. Denali Associates, 3805 Carlson Circle, Palo Alto, CA 94306 Phil F. Brease. In Great Basin Evolution and Metallogeny: Geological Society of Nevada, 2010 Symposium, May 14-22 (Vol. 1, p. 979). DEStech Publications, Inc.

Csejtey Jr, B., Cox, D.P., Evarts, R.C., Stricker, G.D. and Foster, H.L., 1982. The Cenozoic Denali fault system and the Cretaceous accretionary development of southern Alaska. Journal of Geophysical Research: Solid Earth, 87(B5), pp.3741-3754.

Darin, M.H., and Dorsey, R.J., 2013, Reconciling disparate estimates of total offset on the southern San Andreas fault: Geology, v. 31, p. 975-988

Eberhart-Phillips, D., Haeussler, P.J., Freymueller, J.T., Frankel, A.D., Rubin, C.M., Craw, P., Ratchkovski, N.A., Anderson, G., Carver, G.A., Crone, A.J. and Dawson, T.E., 2003. The 2002 Denali fault earthquake, Alaska: A large magnitude, slip-partitioned event. Science, 300(5622), pp.1113-1118.

Elliot, J., Freymueller, J.T., and Larsen, C.F., 2013, Active tectonics of the St. Eliaas orogeny, Alaska, observed with GPS measurements: Journal of Geophysical Research: Solid Earth, v. 118, p. 5625-5642.

Ernst, R., and Bleeker, W., 2010, Large igneous provinces (LIPs), giant dyke swarms, and mantle plumes: significance for breakup events within Canada and adjacent regions from 2.5 Ga to the present: Canadian Journal of Earth Sciences, v. 47, p. 695-739.

Fitzgerald, P.G., Sorkhabi, R.B., Redfield, T.F., and Stump, E., 1995, Uplift and denudation of the central Alaska Range: A case study in the use of apatite fission track thermochronology to determine absolute uplift parameters: Journal of Geophysical Research, v. 100, p. 20175-10191.

Fitzgerald, P.G., Sorkhabi, R.B., Redfield, T.F., and Stump, E., 1995, Uplift and denudation of the central Alaska Range: A case study in the use of apatite fission track thermochronology to determine absolute uplift parameters: Journal of Geophysical Research, v. 100, p. 20175-10191.

Frizzell, V.A., Mattinson, J.M., and Matti, J.C., 1986, Distinctive Triassic megaporphyritic monzogranite: Evidence for only 160 km offset along the San Andreas Fault, southern California: Journal of Geophysical Research, v. 91, p. 14,080-14,088.

Frost, B.R., and Frost, C.D., 2008, A geochemical classification for feldspathic igneous rocks: Journal of Petrology, v. 49, p. 1955-1969.

Garver, J.I., Davidson, C.M., 2015, Southwestern Laurentian zircons in upper Cretaceous Flysch of the Chugach-Prince William Terrane in Alaska: American Journal of Science, v. 315, p. 537-556.

Haeussler, P.J., Matmon, A., Schwartz, D.P. and Seitz, G.G., 2017. Neotectonics of interior Alaska and the late Quaternary slip rate along the Denali fault system. Geosphere, 13(5), pp.1445-1463.

Hildebrand R.S., 2015, Dismemberment and northward migration of the Cordilleran orogeny: Baja-BC resolved: GSA Today, v. 25, n. 11, p. 4-11.

Hreinsdottir, S., Freymueller, J.T., Fletcher, H.J., Larsen, C.F., and Burgmann, R., 2003, Coseismic slip distribution of the 2002 M_w 7.9 Denali fault earthquake, Alaska, determined from GPS measurements: Geophysical Research Letters, v. 30, p.1670-1673.

Hung, C.-H., 2008, Zircon U-Pb Ages and Geochemical Characteristics of the McKinley Sequence and Associated Plutons, Central Alaska Range: M.S. Thesis, National Taiwan University, 78 p.

James, E.W., 1992, Cretaceous metamorphism and plutonism in the Santa Cruz Mountains, Salinian block, California, and correlation with the southernmost Sierra Nevada: Geological Society of America Bulletin, v. 104, p. 1326-1339.

Jicha, B.R., Scholl, D.W., Singer, B.S., and Yogodzinski, G.M., 2006, Revised age of Aleutian Island Arc formation implies high rate of magma production: Geology, v. 34, p. 661-664.

Lanphere, M.A., and Reed, B.L., 1985, The McKinley sequence of granitic rocks; A key element in the accretionary history of southern Alaska: Journal of Geophysical Research, v. 90, p. 11413-11430.

Lease, R.O., Haeussler, P.J. and O'Sullivan, P., 2016. Changing exhumation patterns during Cenozoic growth and glaciation of the Alaska Range: Insights from detrital thermochronology and geochronology. Tectonics, 35(4), pp.934-955.

Lowey, G.W., 1998. A new estimate of the amount of displacement on the Denali fault system based on the occurrence of carbonate megaboulders in the Dezadeash Formation (Jura-Cretaceous), Yukon, and the Nutzotin Mountains sequence (Jura-Cretaceous), Alaska. Bulletin of Canadian Petroleum Geology, 46(3), pp.379-386.

Mahan, K.H., and Williams, M.L., 2005, Reconstruction of a large deep-crustal terrane: Implication for the Snowbird tectonic zone and early growth of Laurentia: Geology, v. 33, n. 5, p. 385-388, doi:10.1130/G21273.1.

Matmon, A., Schwartz, D.P., Haeussler, P.J., Finkel, R., Lienkaemper, J.J., Stenner, H.D. and Dawson, T.E., 2006. Denali fault slip rates and Holocene–late Pleistocene kinematics of central Alaska. Geology, 34(8), pp.645-648.

Mezger, J.E., 1997. Tectonometamorphic evolution of the Kluane metamorphic assemblage, SW Yukon: evidence for Late Cretaceous eastward subduction of oceanic crust underneath North America (Doctoral dissertation, University of Alberta).

Miller, M.L., Bradley, D.C., Bundtzen, T.K. and McClelland, W., 2002. Late Cretaceous through Cenozoic strike-slip tectonics of southwestern Alaska. The Journal of Geology, 110(3), pp.247-270.

Miyashiro, A., 1974, Volcanic rock series in island arcs and active continental margins: American Journal of Science, v. 274, p. 321-355.

Molnar, P. and Dayem, K.E., 2010. Major intracontinental strike-slip faults and contrasts in lithospheric strength. *Geosphere*, *6*(4), pp.444-467.

Nokleberg, W.J., Jones, D.L. and Silberling, N.J., 1985. Origin and tectonic evolution of the Maclaren and Wrangellia terranes, eastern Alaska Range, Alaska. Geological Society of America Bulletin, 96(10), pp.1251-1270.\

Phillips, R.J., Searle, M.P., and Parrish, R.R., 2013, The geochemical and temporal evolution of the continental lithosphere and its relationship to continental-scale faulting: The Karakoram Fault, eastern Karakoram, NW Himalayas: Geochemistry, Geophysics, and Geosystems, v. 14, p. 583-603.

Powell, R.E., 1993, Balanced palinspastic reconstruction of pre-late Cenozoic Paleogeology, southern California: Geologic and kinematic constraints on evolution of the San Andreas fault system: in Powell, R.E., et al. eds., The San Andreas fault system: Displacement, palinspastic reconstruction, and geologic evolution: Geological Society of America Memoir 178, p. 1-106.

Reed, B.L., and Lanphere, M.A., 1974, Offset plutons and history of movement along the McKinley segment of the Denali fault system, Alaska: Geological Society of America Bulletin, v. 85, p. 1883-1892

Riccio, S.J., Fitzgerald, P.G., Benowitz, J.A. and Roeske, S.M., 2014. The role of thrust faulting in the formation of the eastern Alaska Range: Thermochronological constraints from the Susitna Glacier thrust fault region of the intracontinental strike-slip Denali fault system. Tectonics, 33(11), pp.2195-2217.

Ridgway, K.D., Thoms, E.E., Layer, P.W., Lesh, M.E., White, J.M. and Smith, S.V., 2007. Neogene transpressional foreland basin development on the north side of the central Alaska Range, Usibelli Group and Nenana Gravel, Tanana basin. Special Paper of the Geological Society of America, (431), pp.507-547.

Ridgway, K.D., Trop, J.M., Nokleberg, W.J., 2002. Mesozoic and Cenozoic tectonics of the eastern and central Alaska Range: progressive basin development and deformation in a suture zone. Geol. Soc. Am. Bull. 114 (12), 1480–1504.

Roeske, S.M., Benowitz, J.A., Huff, C., Riccio, S., Fitzgerald, P.G., Perry, S.E. and Layer, P.W., 2011, October. Variable strain partitioning with depth along the dextral Denali Fault in the eastern Alaska Range. In Geological Society of America Abstracts with Programs.

Rosenberg, C. L., 2004, Shear zones and magma ascent: A model based on a review of the Tertiary magmatism in the Alps: Tectonics, v. 23, TC3002, doi:10.1029/2003TC001526.

Roman-Berdiel, T., Gapais, D., and Brun, J.-P., 1997, Granite intrusion along strike-slip zones in experiment and nature: American Journal of Science, v. 297, p. 651-678.

Shui, X., He, Z., Klemd, R., Zhang, Z., Lu, T., Yan, L., 2018, Early Jurassic adakitic rocks in the southern Lhasa sub-terrane, southern Tibet: petrogenesis and geodynamic implications: Geological Magazine: v. 155, p. 132-148.

Sutherland, R., 1999, Cenozoic bending of New Zealand basement terranes and Alpine Fault displacement: A brief review: New Zealand Journal of Geology and Geophysics: v. 42, p. 295-301.

Tait, L.D., 2017. Strain and Vorticity Analysis of Mid-Crustal Rocks Exhumed Along the Denali Fault in the Eastern Alaska Range. University of California, Davis.

Tikoff and Teyssier, 1992, Crustal-scale, enechelon “P-shear” tensional bridges: A possible solution to the batholithic room problem: Geology, v. 20, p. 927-930.

Toeneboehn, K., Cooke, M.L., Bernis, S.P., Fendick, A.M., and Benowitz, J., 2018, Stereovision combined with particle tracking velocimetry reveals advection and uplift within a restraining bend simulating the Denali Fault: Frontiers in Earth Science, v. 6, n. 152.

Trop, J.M., Benowitz, J., Cole, R.B. and O'Sullivan, P., 2019. Cretaceous to Miocene magmatism, sedimentation, and exhumation within the Alaska Range suture zone: A polyphase reactivated terrane boundary. Geosphere, 15(4), pp.1066-1101.

Trop, J.M., Ridgway, K.D. and Sweet, A.R., 2004. Stratigraphy, palynology, and provenance of the Colorado Creek basin, Alaska, USA: Oligocene transpressional tectonics along the central Denali fault system. Canadian Journal of Earth Sciences, 41(4), pp.457-480.

Trop, J., Benowitz, J., Cole, R., and O'Sullivan, P., in press, Cretaceous to Miocene magmatism, sedimentation, and exhumation within the Alaska Range suture zone: A polyphaser reactivated terrane boundary: Accepted to Geosphere.

Umhoefer, P.J., 2000, Where are the missing faults in translated terranes?: Tectonophysics, v. 326, p. 23-35.

Waldien, T.S., Roeske, S.M., Benowitz, J.A., Allen, W.K., Ridgway, K.D. and O'Sullivan, P.B., 2018. Late Miocene to Quaternary evolution of the McCallum Creek thrust system, Alaska: Insights for range-boundary thrusts in transpressional orogens. Geosphere, 14(6), pp.2379-2406.

FIGURE CAPTIONS

Figure 1: **S**implified tectonic map of southern Alaska on a shaded relief base with existing Denali Fault geologic constraints of offset and slip rate calculations (modified from Fitzgerald et al. (2014). Pleistocene slip rates from Haeussler et al. (2017)). HCf: Hines Creek Fault; Tf: Totschunda Fault; Taf: Talkeetna Fault; WVf: Wrangell Volcanic field; CMf: Castle Mountain fault; BRf: Border Ranges fault; Ff: Fairweather fault

Figure 2: Simplified geologic map of the Denali Fault modified after Reed and Lanphere (1974) showing interpreted offset between Foraker and McGonagall plutons and drainage divides for the modern river detrital samples. Sample locales are shown, and available in DR1. Inset in upper left shows location in relation to the

northern Cordillera. Inset in lower right shows detrital zircon U-Pb geochronologic results from modern river sediments draining both the Foraker and McGonagall plutons given as probability density plots.

Figure 3: Field photograph of the McGonagall pluton adjacent to the north side of glaciated Denali Fault. Denali Fault covered by the Muldrow Glacier. Field photo location is Gunsight pass and noted on Fig. 2.

Figure 4: Representative photomicrographs from Foraker (upper photo) and McGonagall (lower) plutons. Notice coarse K-feldspar in Foraker sample where the McGonagall is dominated by plagioclase, often preserving oscillatory zonation. Scale bar in both photographs is 1 mm.

Figure 5: Summary of geochemical results. A-B) Fe-index (A) and modified alkali lime index (B) plots (after Frost and Frost (2008)) showing new data from Foraker and McGonagall plutons as well as original data presented by Reed and Lanphere (1974) – note the magnesian and calcic nature of both plutons consistent with an oxidized and high temperature origin; C) Chondrite-normalized REE diagram (Sun and McDonough, 1989) for the McGonagall and Foraker plutons (note slope differences and Eu anomaly present in Foraker samples); D) incompatible element diagram (Sun and McDonough, 1989) showing similar patterns in both Foraker and McGonagall plutons consistent with an arc origin, but the McGonagall pluton has a strong positive Sr anomaly and contains other attributes similar to adakitic rocks derived from lower-crustal sources.

Figure 6: A) False-colored cathodoluminescence image of representative zircon from the Foraker pluton showing oscillatory zonation and doubly terminated geometry consistent with an igneous origin; B) Tera-Wasserburg plots from four samples from the Foraker pluton (see Figure 2). Note that the two samples of the western Foraker pluton from adjacent to the Denali Fault are significantly older than the remainder of the pluton, and likely correlative with a more widespread intrusive event (McKinley sequence; Lanphere and Reed, 1985); C) $^{206}U/^{238}Pb$ results from two easternmost samples in the Foraker pluton that yielded Eocene results; D) Tera-Wasserburg plots from four samples over $^{206}Pb/^{238}U$ results from all samples from the McGonagall pluton arranged from west to east (note the eastward younging direction). Note that there is no overlap in crystallization age of the two plutonic systems.

Figure 7: Paired U-Pb and Hf isotopic results from Eocene samples from this study and from Hung (2008) with 1 σ error bars shown (error bars for Hung (2008) $\varepsilon_{Hf(T)}$ approximated at 1 epsilon unit) comparing crystallization ages and range in Hf isotopic composition. Note no overlap between the two plutonic rocks, with consistently lower $\varepsilon_{Hf(T)}$ values and older crystallization ages from the McGonagall pluton. These data, in conjunction with detrital zircon and bulk rock geochemical analyses, disprove the long-held Foraker-McGonagall piercing point.

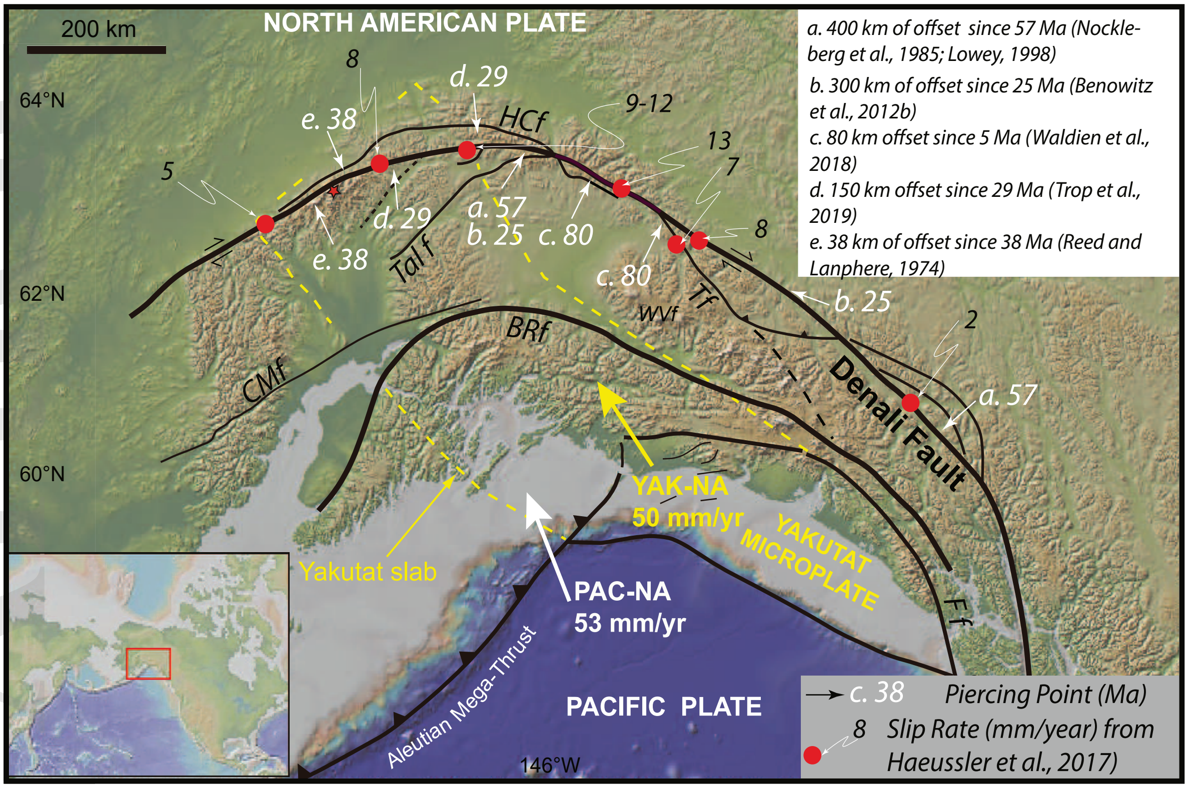
200 km
NORTH AMERICAN PLATE
a. 400 km of offset since 57 Ma (Nockleberg et al., 1985; Lowey, 1998)
b. 300 km of offset since 25 Ma (Benowitz et al., 2012b)
c. 80 km offset since 5 Ma (Waldien et al., 2018)
d. 150 km offset since 29 Ma (Trop et al., 2019)
e. 38 km of offset since 38 Ma (Reed and Lanphere, 1974)
64°N
62°N
60°N
HCf
Tal f
CMf
BRf
WVf
Tf
Ff
Denali Fault
YAK-NA
50 mm/yr
YAKUTAT MICROPLATE
Yakutat slab
PAC-NA
53 mm/yr
PACIFIC PLATE
Aleutian Mega-Thrust
146°W
c. 38 Piercing Point (Ma)
8 Slip Rate (mm/year) from Haeussler et al., 2017)

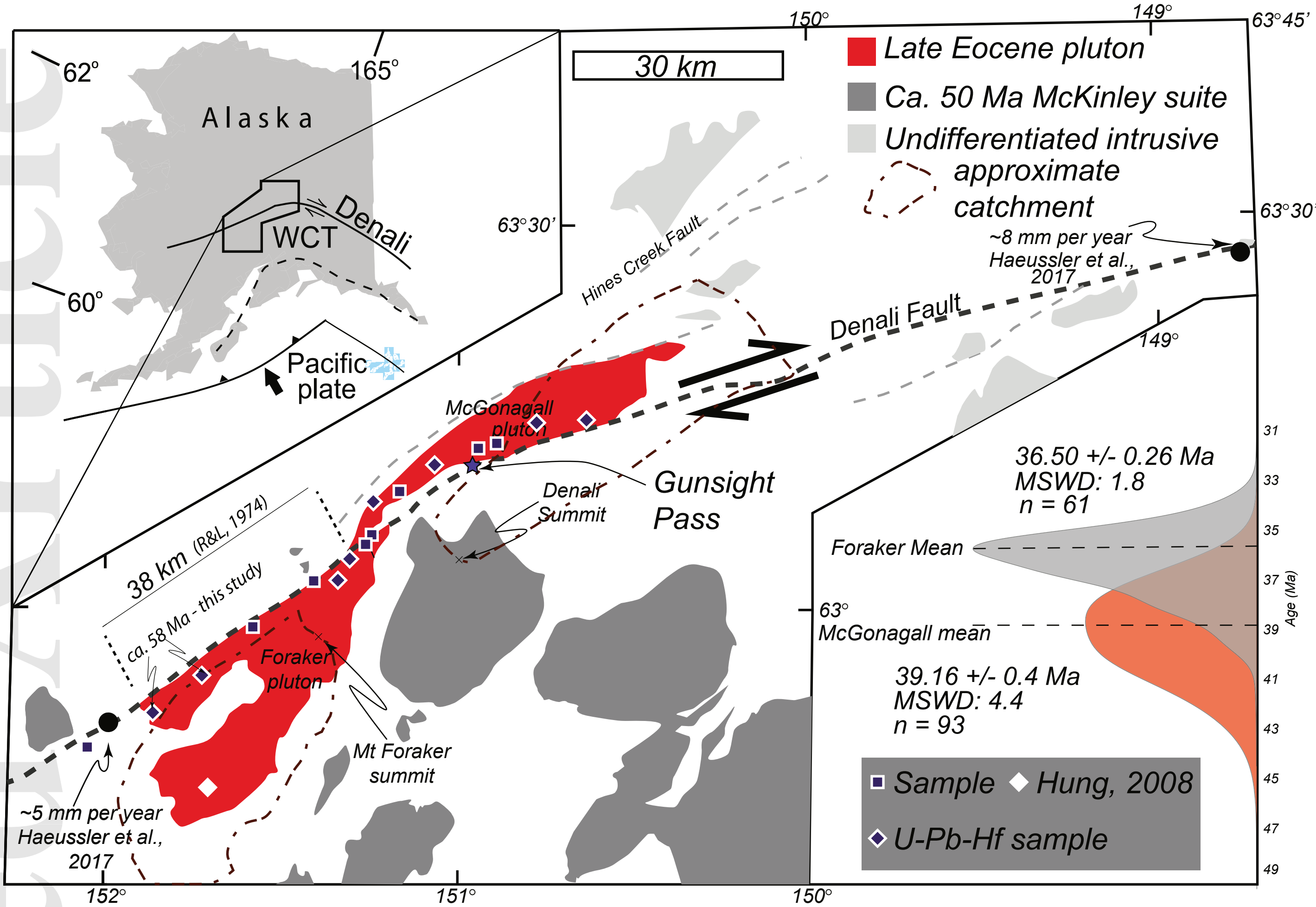

Late Eocene pluton
Ca. 50 Ma McKinley suite
Undifferentiated intrusive
approximate catchment
30 km
Alaska
WCT
Denali
Pacific plate
62°
60°
165°
150°
149°
63°45'
63°30'
63°
152°
151°
Hines Creek Fault
Denali Fault
~8 mm per year Haeussler et al., 2017
~5 mm per year Haeussler et al., 2017
McGonagall pluton
Foraker pluton
Gunsight Pass
Denali Summit
Mt Foraker summit
38 km (R&L, 1974)
ca. 58 Ma - this study
36.50 +/- 0.26 Ma
MSWD: 1.8
n = 61
Foraker Mean
McGonagall mean
39.16 +/- 0.4 Ma
MSWD: 4.4
n = 93
Age (Ma)
Sample
Hung, 2008
U-Pb-Hf sample


McGonagall
Pluton
Muldrow
Glacier
Denali Fault zone

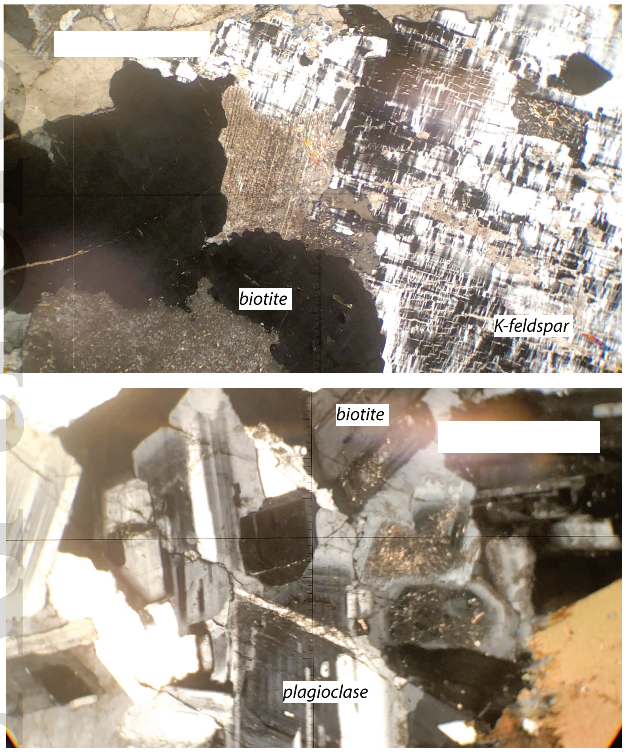
biotite
K-feldspar
biotite
plagioclase

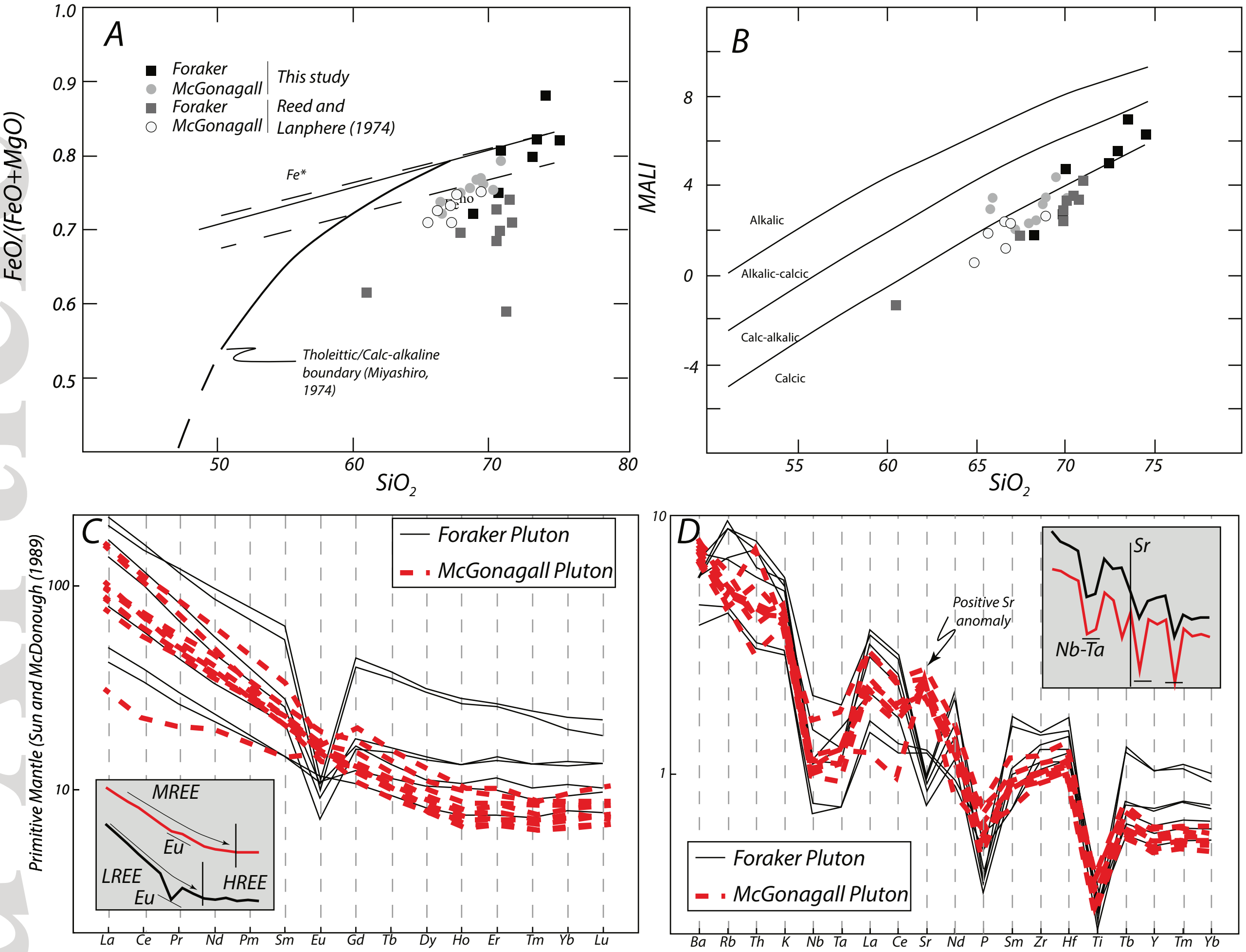
A
Foraker
McGonagall
This study
Foraker
McGonagall
Reed and Lanphere (1974)
Fe*
Tholeittic/Calc-alkaline boundary (Miyashiro, 1974)
FeO/(FeO+MgO)
SiO2
B
Alkalic
Alkalic-calcic
Calc-alkalic
Calcic
MALI
SiO2
C
Foraker Pluton
McGonagall Pluton
Primitive Mantle (Sun and McDonough (1989)
MREE
Eu
LREE
Eu
HREE
La Ce Pr Nd Pm Sm Eu Gd Tb Dy Ho Er Tm Yb Lu
D
Positive Sr anomaly
Sr
Nb-Ta
Foraker Pluton
McGonagall Pluton
Ba Rb Th K Nb Ta La Ce Sr Nd P Sm Zr Hf Ti Tb Y Tm Yb

ter_12437_f6.pdf

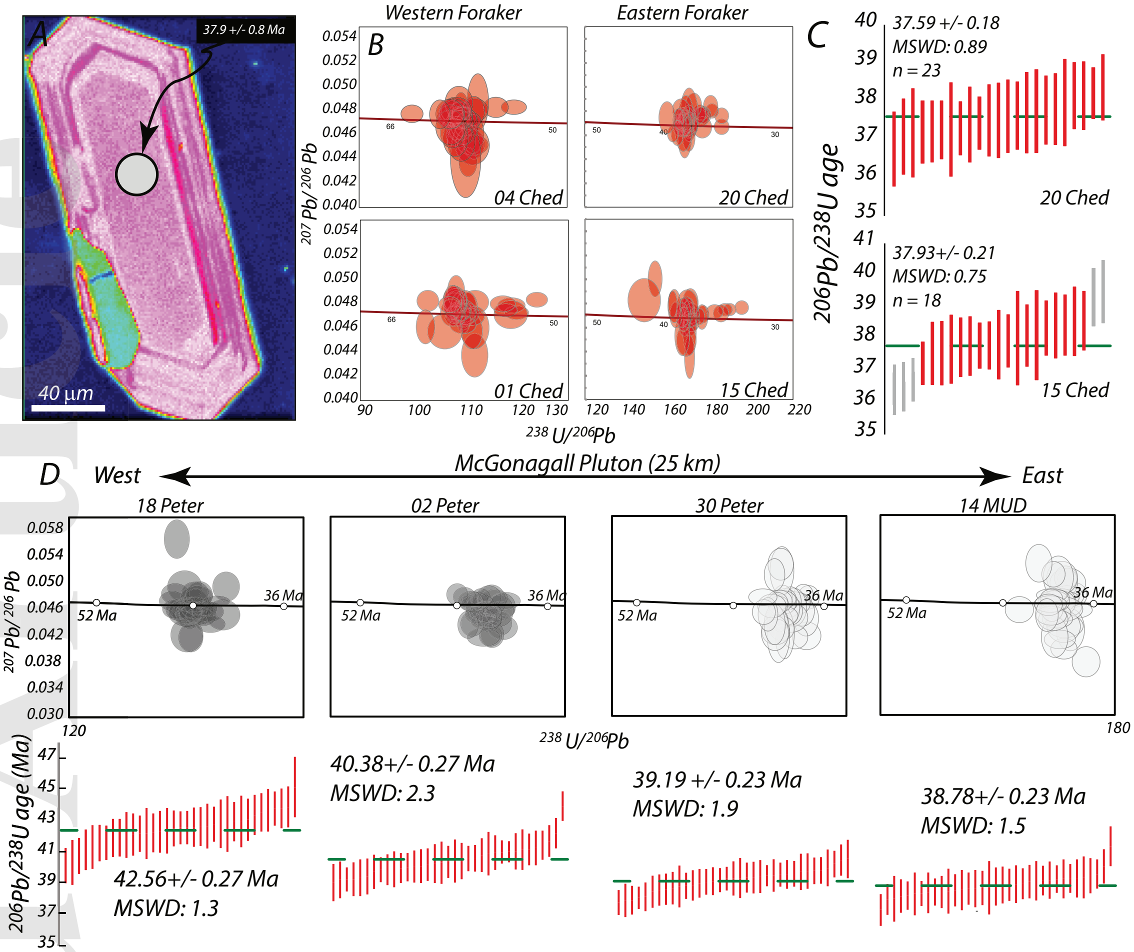

ter_12437_f7.pdf